RSC Advances

PAPER

View Article Online
View Journal | View Issue

Cite this: *RSC Adv.*, 2024, **14**, 8018

Citric acid cross-linking of a hydrogel from *Aloe vera* (*Aloe barbadensis* M.) engenders a pH-responsive, superporous, and smart material for drug delivery

Jaffar Irfan,[a] Arshad Ali,[a] Muhammad Ajaz Hussain, *[b] Muhammad Tahir Haseeb,[c] Muhammad Naeem-ul-Hassan [a] and Syed Zajif Hussain [d]

The current research work is based on the evaluation of a citric acid (CA) cross-linked *Aloe vera* (*Aloe barbadensis* M.) leaf hydrogel (CL-ALH) for pH-dependent and sustained drug release application. The CA was used in different concentrations (1.25, 2.5, 5.0, and 10.0%) to cross-link the ALH using homogenous reaction conditions. The synthesis of CL-ALH was confirmed through Fourier transform and nuclear magnetic resonance spectroscopic studies. The thermal analysis indicated that the ALH and CL-ALH were stable and decomposed in two steps. The scanning electron microscopic images of CL-ALH confirmed its porous nature due to the presence of interconnected channeling. The swelling of CL-ALH was evaluated at pH 1.2, 6.8, and 7.4 as well as in deionized water (DW). High swelling of CL-ALH was observed in DW, and at pH 7.4 and 6.8 whereas, less swelling of CL-ALH was witnessed at pH 1.2. CL-ALH also exhibited swelling/deswelling behavior in DW and ethanol, DW and normal saline, and at pH 7.4 and 1.2. Tablets were prepared from CL-ALH as a release retarding agent demonstrating the sustained release of venlafaxine hydrochloride (VFX) for 8 h. Whereas, VFX was released within 4 h from the ALH-based tablet formulation (un-cross-linked material) indicating the prolonged and sustained release behavior of CL-ALH. The VFX was released from CL-ALH tablets and followed zero-order kinetics. The mechanism followed by VFX release from CL-ALH tablets was non-Fickian diffusion. The *in vivo* fate of the tablet formulation was observed through an X-ray study. The CL-ALH-based tablet safely passed through the stomach of a stray dog without any significant erosion and then disintegrated in the small intestine and colon. These findings confirmed that the CL-ALH is an effective excipient for designing a sustained-release drug delivery system for the small intestine and colon.

Received 4th January 2024
Accepted 26th February 2024

DOI: 10.1039/d4ra00095a

rsc.li/rsc-advances

1. Introduction

Naturally occurring plant-based materials are catching the eyes of many researchers for their utilization in the biomedical field day by day owing to their non-toxicity, biocompatibility, biodegradability, non-hemolytic, and non-immunogenicity.[1–4] These polysaccharides have many functional groups which are being used for physical and chemical cross-linking.[5,6] Through cross-linking, the physical and chemical properties of polysaccharides are tuned to get desired results or applications.[7,8] After cross-linking, the stimuli-responsive swelling (pH, temperature, ions, solvent, electric and magnetic field), mechanical strength, and targeted and sustained drug release profile can be induced or improved.[9–11]

Cross-linking of polysaccharides is also helpful in developing and utilizing such materials in conventional and benign drug delivery systems (DDSs).[12–14] Many synthetic and semi-synthetic cross-linkers are being used for the cross-linking of polysaccharides, *i.e.*, glutaraldehyde, oxalyl chloride, glyoxal, dextrin, epichlorohydrin, borax, citric acid (CA), *etc.*[15] Among these cross-linkers, CA is recognized as an economical, non-toxic, and green agent used for the cross-linking of polysaccharides.[16,17]

Aloe vera (Syn: *Aloe barbadensis* M.) grows in almost every part of the world, especially in dry areas. Different parts of *A. vera* have a wide range of medicinal applications and, hence, are recognized by ancient Greek scientists as a universal cure-all plant. *A. vera* leaves contain sticky mucilage/hydrogel mainly composed of glucomannan.[18,19] Moreover, acemannan (β-1,4 acetylated mannan) is one of the major polysaccharidal units of the *A. vera* hydrogel which is hydrophilic and used to treat

[a]*Institute of Chemistry, University of Sargodha, Sargodha 40100, Pakistan*
[b]*Centre for Organic Chemistry, School of Chemistry, University of the Punjab, Lahore 54590, Pakistan. E-mail: majaz172@yahoo.com*
[c]*College of Pharmacy, University of Sargodha, Sargodha 40100, Pakistan*
[d]*Department of Chemistry, SBA School of Science & Engineering, Lahore University of Management Sciences, Lahore Cantt. 54792, Pakistan*

wounds. *A. vera* has been utilized in different DDSs, *e.g.*, emulgel,[20] sustained release oral hydrogel disc,[21] nanoparticles,[22] buccal, oral, and transdermal gels,[23] wound dressing,[24,25] *etc.*

In the present research, *A. vera* will be cross-linked with CA to modify the swelling of the *A. vera* hydrogel (ALH) and develop a sustained-release oral tablet formulation following zero-order kinetics. The synthesized CL-ALH will be characterized through spectroscopic and analytical techniques. The thermal stability of ALH before and after cross-linking will be tested by performing the thermal analysis. The surface morphology of CL-ALH will be appraised through scanning electron microscopy (SEM). This research work will emphasize the determination of pH-responsive swelling, stimuli-responsive swelling/deswelling, and sustained drug release profile. The *in vivo* fate of the CL-ALH-based tablet after its administration to the dog will be observed through an X-ray study of the gastrointestinal tract (GIT).

2. Materials and methods

2.1. Materials

Fresh plant leaves of *A. vera* were acquired from a local marketplace of district Sargodha, Sargodha, Pakistan. *A. vera* plant leaves were cleaned manually by washing with DW and cut into small pieces. The transparent gel was isolated from the internal walls of *A. vera* leaf and washed with *n*-hexane. The *A. vera* hydrogel (ALH) was dried in an oven and stored in a desiccator. Reagents and chemicals were of analytical grade and used as such without further purification. Potassium dihydrogen phosphate, *N*,*N*-dimethylacetamide (DMAc), 4-dimethylaminopyridine (DMAP), barium sulphate, *n*-hexane, ethanol, calcium chloride ($CaCl_2$), NaCl, KCl, and HCl were provided by Riedel-de Haën, Germany. Oxalic acid was used to standardize NaOH and both of these chemicals were procured from Merck Chemicals GmbH, Darmstadt, Germany. The citric acid (CA) was obtained from Fischer Scientific, USA. Polyvinyl pyrrolidone (PVP) and magnesium stearate was purchased from Sigma-Aldrich Co., (St. Louis, MO, USA). Venlafaxine HCl (VFX, European Pharmacopoeia standard) was used to monitor the sustained release potential of the benign material, *i.e.*, CA cross-linked *A. vera* hydrogel (CL-ALH). The experimental work was performed using deionized water (DW).

2.2. Extraction of ALH

A. vera plant leaves were cleaned manually, washed with DW, and chopped into small pieces to separate the mucilage/hydrogel (ALH) present in their inner sides with the help of a knife. The ALH was washed with DW and *n*-hexane to eradicate polar and non-polar impurities, respectively. The ALH after purification was spread on a steel tray. It was then dried in an oven at 55 °C for 24 h. After drying, the ALH was milled and passed through a mesh no. 40 to get its finely divided form. Finally, ALH was stored in a desiccator before its utilization in further experimental work.

2.3. Synthesis of CL-ALH

To cross-link ALH with CA, the method given in ref. 11 was used with slight modification. Briefly, ALH (2.0 g) was suspended in DMAc (50 mL) for 2 h at 80 °C. The suspension of ALH and DMAc was stirred at 250 rpm. A solution of CA in DW (5% *w*/*v*) was prepared and mixed in the suspension of ALH and DMAc. To enhance the rate of reaction, DMAP (50 mg) was added as a catalyst and the reaction was further continued for 24 h at 80 °C. The obtained material (CL-ALH) was precipitated in methanol (150 mL), washed with DW, vacuum dried at 60 °C, and milled to get powder form. The CL-ALH was saved in a container to use in the experimental work. Alike procedure was opted to prepare CL-ALH derivatives using 1.25, 2.5, and 10% CA. However, after evaluation of some primary studies, *i.e.*, yield, degree of substitution, and swelling properties in DW, it was noted that CL-ALH prepared with 5% CA was good enough to use for further experimentaion. Therefore, this derivative was further upsized to study all of the work being reported here.

2.4. Measurements

The FTIR (KBr) spectra of ALH and CL-ALH were recorded on an IRPrestige-20 spectrophotometer (Shimadzu, Japan) in the range from 4000 to 400 cm^{-1}. The samples of both materials in thin pellet form were prepared by mixing them with KBr followed by compression under hydraulic pressure. The solid-state NMR (CP/MAS ^{13}C NMR) spectra of the ALH and CL-ALH were recorded at ambient temperature on a Bruker DRX-400 machine. The thermal stability of ALH before and after cross-linking with CA was studied by performing thermogravimetric analysis (TGA) and recording thermal decomposition temperatures using SDT Q600 thermal analyzer (TA Instruments, USA). The TG curves of ALH and CL-ALH were recorded at the onset of 10 °C min^{-1} from ambient temperature to 800 °C under nitrogen. The SEM images of CL-ALH were recorded in swollen then freeze-dried form using a Scanning Electron Microscope (SEM; Nova, NanoSEM 450).

2.5. Swelling studies of CL-ALH

The ability of CL-ALH to swell in DW and at pH 1.2, 6.8, and 7.4 was studied using tea-bag method (gravimetric). CL-ALH (100 mg) was packed in wet tea-bags and hung in the beakers (100 mL) having swelling media for 300 min. After certain periods, the tea-bags holding the swelled CL-ALH were removed from the beakers, and the excess swelling media were drained. The tea-bag was weighed accurately and the swelling capacity was calculated using eqn (1). The swelling of CL-ALH was studied till equilibrium, *i.e.*, 300 min.

$$\text{Swelling of CL-ALH } \left(\text{g g}^{-1}\right) = \frac{W_t - W_c - W_o}{W_o} \quad (1)$$

where, W_t (g), W_c (g), and W_o (g) represented the tea-bag weight of CL-ALH (swelled), wet empty tea-bag, and CL-ALH (dry), respectively.

2.6. Swelling kinetics of CL-ALH

From the swelling studies of CL-ALH in DW and at different physiological pH, CL-ALH's absorption rate of swelling media

and the extent of its swelling in terms of the normalized degree of swelling (Q_t) (eqn (2)) and normalized equilibrium degree of swelling (Q_e) (eqn (3)) were calculated.

$$Q_t = \frac{W_S - W_D}{W_D} = \frac{W_T}{W_D} \quad (2)$$

$$Q_e = \frac{W_\infty - W_D}{W_D} = \frac{W_E}{W_D} \quad (3)$$

where W_D indicated the weight of CL-ALH (dry) at time, $t = 0$, and W_s showed the weight of the CL-ALH (swelled) at time t. W_T is the weight of swelling medium entrapped into the CL-ALH at time t. W_∞ is the weight of CL-ALH (swelled) after t_∞ time. W_E is the weight of swelling medium remaining in the CL-ALH at time, $t = \infty$.

By plugging the values of Q_e and Q_t into the eqn (4), the swelling kinetics (second-order) of CL-ALH was calculated.

$$\frac{t}{Q_t} = \frac{t}{Q_e} - \frac{1}{kQ_e^2} \quad (4)$$

2.7. Saline-responsive swelling of CL-ALH

Solutions of different molar strengths from 0.1 to 2 M of both NaCl and KCl were prepared in DW to evaluate the saline-dependent swelling of CL-ALH. The CL-ALH (100 mg) was taken and packed in each of the 8 tea-bags. The tea-bags were suspended in the saline solutions and swelling indices were determined in each salt solution after 24 h at room temperature.

2.8. Swelling/deswelling studies behavior of CL-ALH

In the investigation of the swelling/deswelling behavior of CL-ALH, the tea-bag method, which was mentioned above, was used. After adding 100 mg of CL-ALH to the tea-bag, it was hung upside down in a beaker containing 100 mL of swelling medium, *i.e.*, pH 7.4, and allowed to expand for 1 h. The weight of the tea-bag was determined using eqn (1) after every 15 min. After 1 h of studying the effects of swelling, the same tea-bag was placed in a different beaker (100 mL) that contained a deswelling medium, *i.e.*, pH 1.2, and it was left to deswell for 1 h. After waiting for 15 min., the tea bag was removed and its ability to deswell was determined using eqn (1). This cycle of swelling/deswelling was performed a total of four times. Using the same methodology, the swelling/deswelling behavior of CL-ALH in DW and ethanol as well as in DW and normal saline (0.9% aqueous NaCl solution) was also determined.

2.9. Preparation of tablets

CL-ALH sustained release capabilities for the oral DDS were evaluated using VFX as a model drug. Already reported technique for preparing a CL-ALH-based oral tablet formulation (CL-ALHT) was used.[26] The 250 mg of CL-ALH and 100 mg of VFX were mixed and homogenized. The mixture of CL-ALH and VFX was moisturized with the solution of PVP-K30 in DW (5% w/v). The produced wet material was dried in a vacuum oven (50 °C), passed through a mesh size of 20, and then lubricated with magnesium stearate (5 mg). Tablets having a hardness of 6.5–7.5 kg cm^{-2} were produced by compressing the granules on a rotary press using a 9 mm flat surface punch. Similar concentrations of all ingredients (except CL-ALH, replaced with the same amount of ALH) were used to prepare only ALH-based tablets (ALHT) for the drug release comparison between CL-ALH and ALH-based tablets.

2.10. *In vitro* venlafaxine release study

USP Dissolution Apparatus II was used to conduct an *in vitro* VFX release study from VFX tablets (CL-ALHT and ALHT) at 50 rpm speed of the paddles and 37 °C temperature. The VFX release study was conducted at pH 6.8 (900 mL) for 8 h. The sample was taken out at regular intervals, and the 900 mL of dissolution medium was regularly replenished with a newly made buffer of pH 6.8. The dissolution sample was passed through a nylon filter (0.45 μm) and diluted (if necessary). To determine how much VFX was released from VFX tablets, DDSolver Software was used to analyze absorbance readings taken at 280 nm on a UV-Vis spectrophotometer (UV-1600 Shimadzu, Germany).

2.11. Drug release kinetics and mechanism

The VFX release kinetics from VFX tablets (CL-ALHT and ALHT) were determined using a zero-order kinetic equation (eqn (5)) and the VFX release mechanism from VFX tablets were determined by power law (eqn (6)).[27,28]

$$Q_t = k_0 t \quad (5)$$

$$\frac{M_t}{M_\infty} = k_p t^n \quad (6)$$

where, k_0 is the zero-order rate constant and Q_t is the quantity of VFX released at time t. The quantity of VFX released at time t is denoted by M_t/M_∞, the Korsmeyer–Peppas constant is k_p, and the diffusion exponent, n, illustrated the VFX release mechanism. The criteria for determining the Fickian diffusion, non-Fickian diffusion, case-II transport, and super case-II transport were as follow: $n < 0.45$, between 0.45 and 0.89, equal to 0.89, and greater than 0.89, respectively.[29,30]

2.12. X-ray study

To determine the fate of tablet formulation of VFX during the transit through the gastrointestinal tract (GIT), a tablet (CL-ALHX) was designed with slight modification as described in Section 2.9. Briefly, a radio opaquant material, *i.e.*, barium sulfate ($BaSO_4$, 25 mg) was added to the tablet formulation for better visualization during the X-ray study. Instead of 100 mg of VFX, 75 mg was used in CL-ALHX to maintain a uniform weight of the tablet. The rest of the procedure for the preparation of the tablet (CL-ALHX) was the same as mentioned in Section 2.9. For the X-ray study, a method reported in the literature was followed.[11] A healthy stray dog (18.5 kg) was selected and acclimatized to the laboratory conditions one week before the start of the X-ray study. A single tablet of CL-ALHX was placed in the

stomach of the overnight fast dog through a gavage tube. The dog had free access to ordinary tap water but refrained from food to avoid any effect on the visualization of the CL-ALHX. X-ray images of the abdomen of the dog were captured using an X-ray machine (Beam Limiting Device, Model TF-6TL-6, Toshiba Corporation, Tokyo, Japan) just before and after the intake of CL-ALHX tablet. This *in vivo* study was approved vide letter No. IREC-2018-76-M, dated May 17, 2018, by the Institutional Animal Ethics Committee (IAEC) of 'The University of Lahore', Pakistan.

3. Results and discussion

3.1. Synthesis of CL-ALH

An illustrated reaction scheme for the synthesis of CL-ALH is presented in Fig. 1. A water molecule from one side of –COOH of CA was removed by heating the CA for 2 h at 80 °C in DMAc and converted to a cyclic anhydride as shown in Fig. 1. The cyclic anhydride is very reactive which further reacted with the hydroxyl (–OH) group of ALH and converted to a monoester, *i.e.*, citrate of ALH. Upon continuous heating under similar reaction conditions, the carboxylic (–COOH) group from the second terminal of CA was also dehydrated and converted to another cyclic anhydride which cross-linked with ALH to form CL-ALH.[11]

3.2. Preliminarily studies of CL-ALH

Using four different CA concentrations (1.25, 2.5, 5.0, and 10.0%), four different derivatives of CL-ALH were synthesized. The yield (78.5%) and degree of substitution (DS), *i.e.*, 2.33 of CL-ALH prepared using 5% of CA were found maximum as compared to other concentrations. The equilibrium swelling of CL-ALH was found in the order of 5% > 2.5% > 10% > 1.25% in DW (Fig. 2). This shows that upon increasing the CA concentration from 1.25 to 5% the equilibrium swelling capacity of CL-ALH was also increased from 25.11 to 38.9 g g^{-1}. The increase in the equilibrium swelling capacity of CL-ALH with the increase in CA concentration was due to the presence of a large number of hydrophilic functional groups coming from CA attachment. Therefore, the hydrogel, *i.e.*, CL-ALH will absorb a high amount of water, and a high equilibrium swelling capacity was noted. However, after 5% of CA concentration, the equilibrium swelling capacity of CL-ALH was decreased owing to the increase of cross-linking density of hydrogel, *i.e.*, CL-ALH. As a result, less amount of water was absorbed by CL-ALH and a decrease in the equilibrium swelling capacity was observed.[31] Therefore, 5% CA was found an ideal concentration for the synthesis of CL-ALH. Hence, the CL-ALH with 5% CA was upsized for further analysis and evaluation for drug delivery applications.

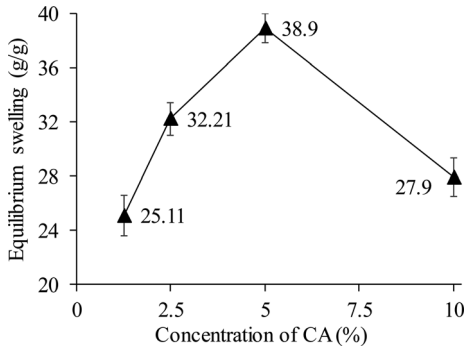

Fig. 2 Equilibrium swelling (g g^{-1}) of CL-ALH prepared from different concentrations of CA.

3.3. Measurements

3.3.1. FTIR analysis. The absorption band at 1612 cm^{-1} in unmodified ALH disappears in CL-ALH as the ester carbonyl signals, due to the successful crosslinking of ALH with CA, appeared at 1728 cm^{-1}.[32] The signals of the polymeric backbone of CL-ALH appeared at 2901 cm^{-1} is due to $-CH_2$ symmetric and –CH stretching vibration whereas the hydroxyl signals in CL-ALH appeared at 3551 cm^{-1}. The stretching vibrations of ether linkage (C–O–C) in ALH spectrum[32] were shifted from 1047 cm^{-1} towards a higher wavenumber, 1081 cm^{-1} after

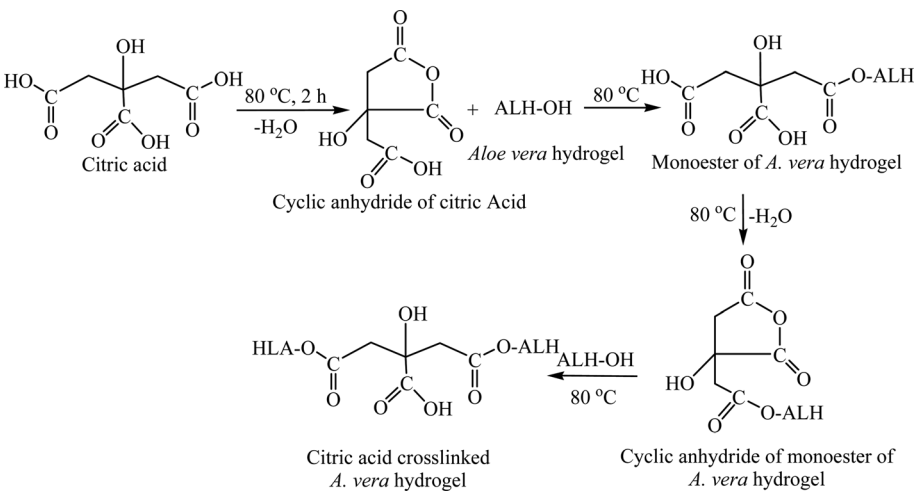

Fig. 1 Illustrated mechanism of the synthesis of CL-ALH.

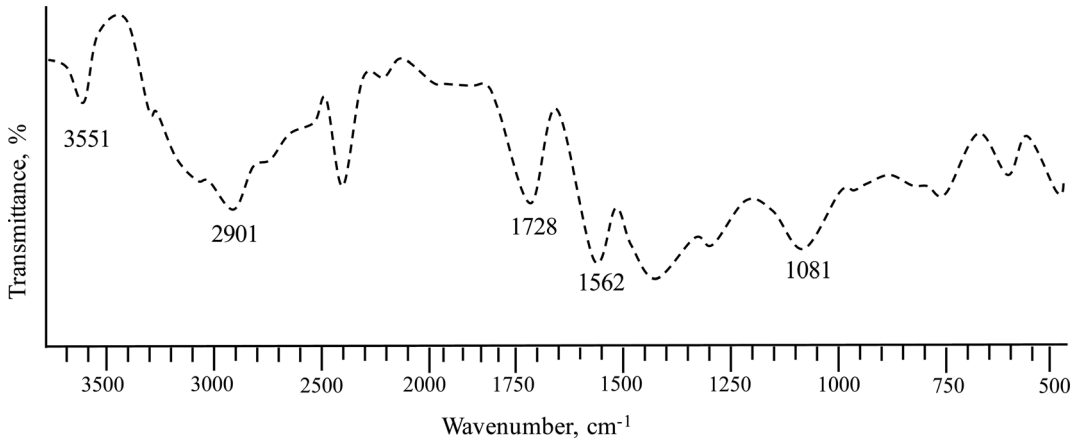

Fig. 3 FTIR spectrum of CL-ALH synthesized using 5% CA.

cross-linking as shown in the FTIR spectrum of CL-ALH (Fig. 3). Similar trends in shifting of C–O–C and ester carbonyl signals are noted for esterifications of relevant biomaterials.[33]

3.3.2. Solid-state CP/MAS ^{13}C NMR analysis. In the solid-state ^{13}C NMR spectrum of CL-ALH (Fig. 4), the signals for C1 appeared at 105.40 ppm and for C2-6 at 62.97 to 84.01 ppm. The signals centered at 174.19 ppm are assigned for C=O groups of CL-ALH. Whereas, the literature has indicated the presence of signals at 105.56 ppm for C1 and 63.24 to 79.33 ppm for C2-6 for unmodified ALH.[32] The upfield shifting in all signals of ALH after crosslinking with CA, especially the carbonyl region indicated the formation of ester bonds between ALH and CA.

3.3.3. Thermal analysis. The TG curves of ALH and CL-ALH revealed that both materials were thermally decomposed in two steps (Fig. 5). The degradation of CL-ALH starts at 230 °C and completes at 355 °C as the first and major degradation step which are higher values than unmodified ALH as seen in Fig. 5. Hence, the comparison of thermal decomposition curves of ALH and CL-ALH indicated that both materials are thermally stable entities. The findings of peers also revealed alike results for CA cross-linking of relevant biomaterials.[11,34]

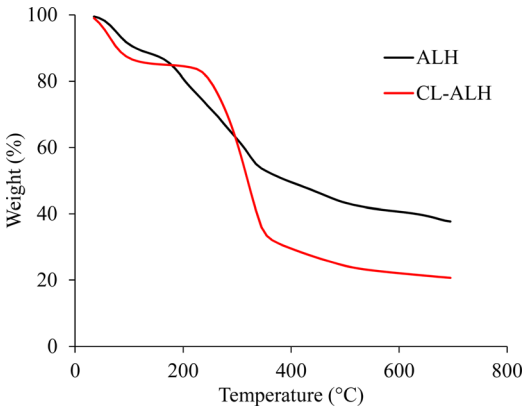

Fig. 5 Overlay TG curve of ALH and CL-ALH.

3.3.4. SEM analysis. Fig. 6 shows the SEM images of the CL-ALH. The interconnected channeling can be seen in the images and reveals its porous nature after cross-linking with CA. The SEM images also revealed that mostly (approximately 60–70%)

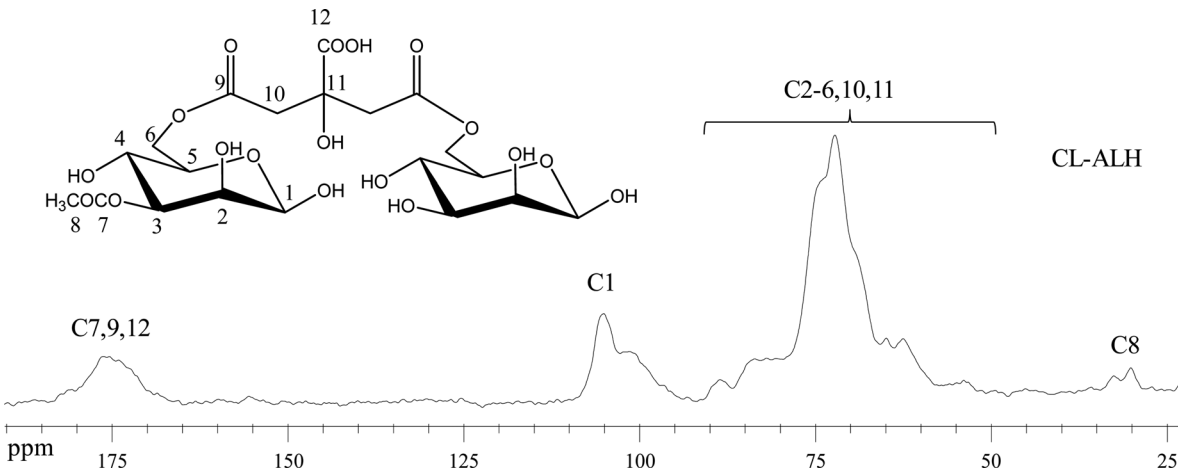

Fig. 4 Solid-state CP/MAS ^{13}C NMR spectrum of CL-ALH.

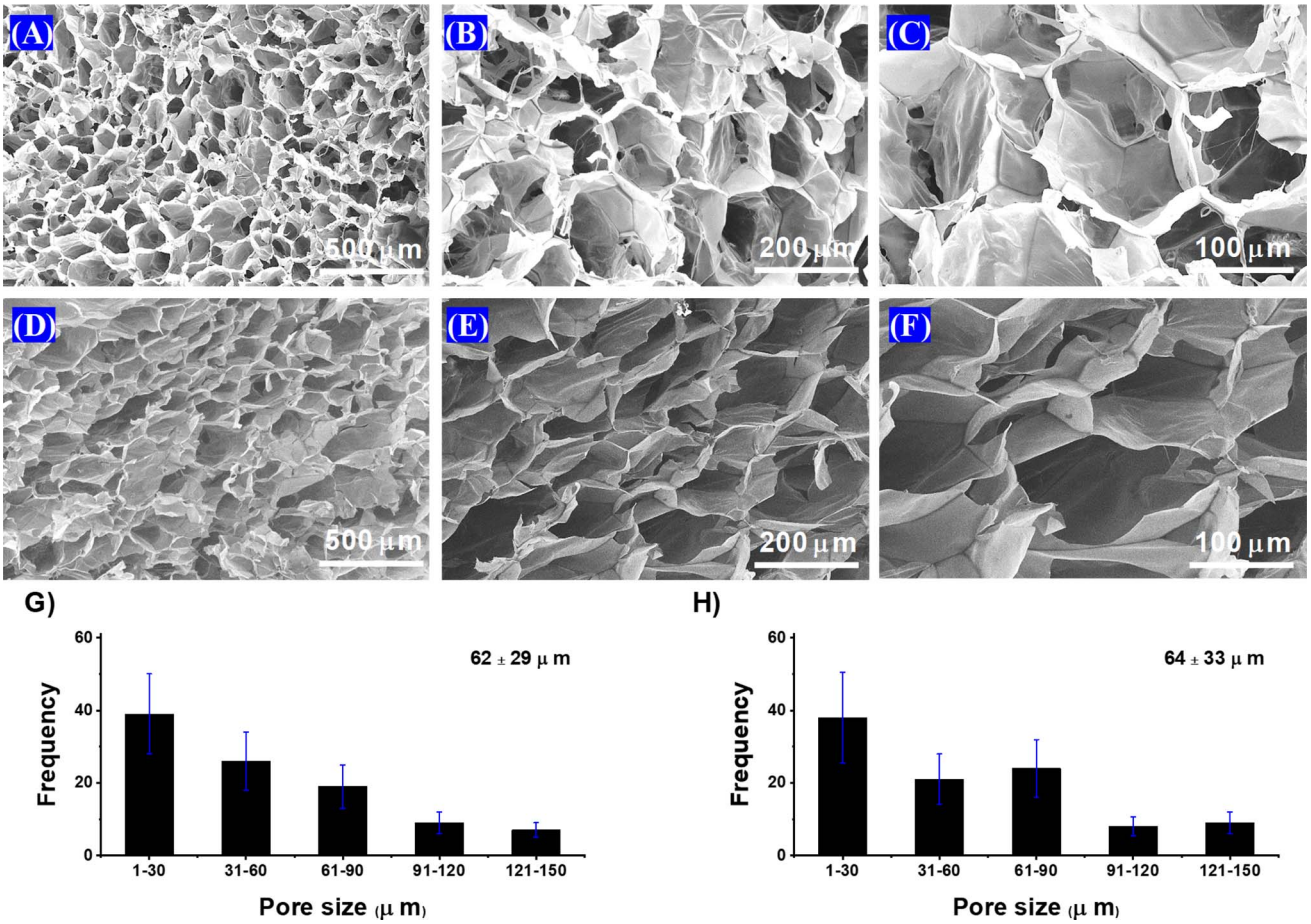

Fig. 6 SEM of CL-ALH (A–C, transverse and D–F, longitudinal) and histogram of CL-ALH (G transverse and H longitudinal).

the pore size of the CL-ALH was observed in the range from 1 to 60 μm both for transverse and longitudinal cross-sectional studies. These findings witnessed that the CL-ALH has the potential to absorb water and other biological fluids and could be a potential material for designing different DDSs. Moreover, there is not a statistically significant difference between different groups of pore size distribution in the histogram.

3.4. Swelling of CL-ALH

The results of the swelling studies of CL-ALH at pH 1.2, 6.8, and 7.4, and in DW are presented in Fig. 7A. It is obvious that the CL-ALH swells extremely well in DW as compared to the other swelling media (pH 1.2, 6.8, and 7.4) during the swelling study of 300 min. At a pH 1.2, the least swelling of the CL-ALH was noted due to the acidic environment of this swelling medium. In an acidic environment, the –COOH groups of the CL-ALH are remained in unionized or protonated form, hence, lacking the anion–anion electrostatic repulsion. As a result, the penetration of the swelling medium becomes difficult and CL-ALH does not swell well at a pH 1.2.[38–40] At pH 6.8 and 7.4, the –COOH groups present in CL-ALH are ionized to form the anions, *i.e.*, $-COO^-$ resulting in the generation of electrostatic repulsions among

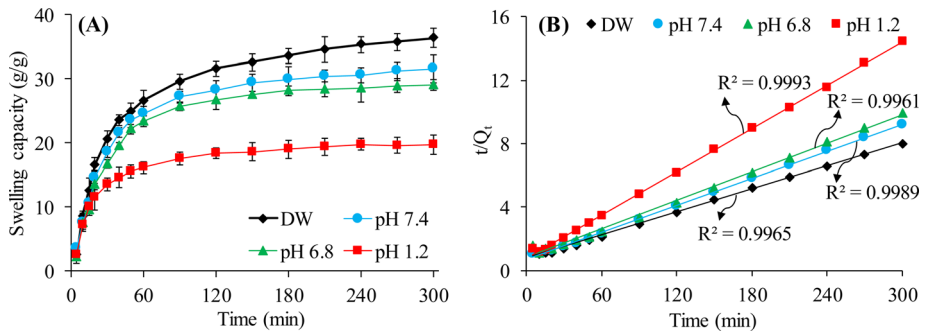

Fig. 7 Swelling capacity (A) and swelling kinetics (B) of CL-ALH in different swelling media.

similar ions. These repulsions push the chains of CL-ALH to move apart from each other due to which the chains get relaxed and uncoiled and allow the swelling media to penetrate. As a result, an increase in the swelling was observed at pH 6.8 and 7.4 as compared to pH 1.2.[35–37] In DW, owing to the absence of any ion and the lack of charge screening effect resulting in the high swelling of CL-ALH as compared to the swelling at pH 6.8 and 7.4. Moreover, it was also noted that the swelling of CL-ALH was more sustained and pronounced at pH 6.8 and 7.4 than that at pH 1.2. This property of CL-ALH will make it a more selective candidate for drug delivery applications.

3.5. Swelling kinetics of CL-ALH

The data of the swelling studies of CL-ALH in different swelling media was used to establish swelling kinetics of CL-ALH. The swelling data of CL-ALH was nicely fitted in the equation of the second-order kinetics model as evidenced by the high value (≈ 1) of R^2 obtained from the straight-line plot between t and slope t/Q_t (Fig. 7B).

3.6. Saline responsiveness of CL-ALH

Fig. 8A indicated the influence of different molar concentrations of NaCl and KCl on the equilibrium swelling properties of CL-ALH for 24 h. The swelling of CL-ALH in different salt solutions was found to decrease rapidly from 18.7 to 15.6 g g^{-1} in NaCl solutions and from 20.4 to 16.9 g g^{-1} in KCl solutions upon increasing the molar concentrations of these salts from 0.1 to 0.5 M (Fig. 8A). This decline in the swelling was due to the presence of the screening effect of the Na^+ and K^+ ions present in the swelling media. Moreover, with the increase in the concentration of salts, the difference in osmotic pressure between the swelling media and CL-ALH increases which is also responsible for the decline in its swelling.[3] In comparison, the CL-ALH swelling was a bit higher in the solutions of KCl than NaCl. This is because of the greater charge density of K^+ ions than Na^+ ions. Therefore, K^+ ions attracted towards $-COO^-$ ions of CL-ALH more rapidly than Na^+ ions which resulted in high swelling in the KCl solution.[8]

3.7. Swelling/deswelling profile of CL-ALH

The pH-dependent swelling/deswelling capacity of CL-ALH has been assessed in pH 7.4 and 1.2 buffers. The rapid increase and decrease in the swelling of CL-ALH was noted at pH 7.4 and 1.2, respectively. Such an increase and decrease in the swelling indicated its swelling/deswelling nature. Similar findings were achieved during four successive swelling/deswelling cycles that demonstrated the reproducibility of pH-responsive swelling/deswelling behavior of CL-ALH (Fig. 8B). In Section 3.4, the reason for the increase and decrease of CL-ALH swelling at pH 7.4 and 1.2, respectively has been explained.

Swelling/deswelling properties of CL-ALH were determined in DW/normal saline (Fig. 8C). CL-ALH possessed higher swelling in DW and exhibited deswelling when dipped in normal saline because of the presence of screening effect of the Na^+ ions. Furthermore, the removal of water from swollen CL-ALH is due to the osmotic pressure difference between CL-ALH and surrounding normal saline.[17] After repeating the same cycle of swelling/deswelling for four times, CL-ALH continues showing its saline-responsive swelling/deswelling properties.

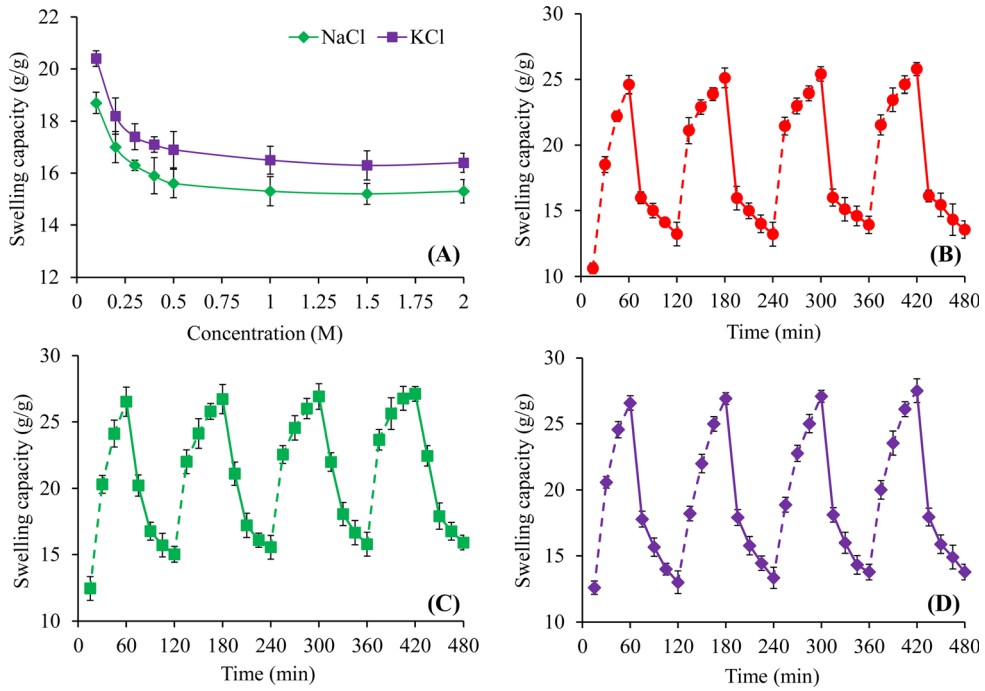

Fig. 8 Saline responsive swelling of CL-ALH (A) and swelling/deswelling behavior of CL-ALH at pH 7.4 and 1.2 (B), DW and 0.9% (w/v) NaCl solution (C), and DW and ethanol (D).

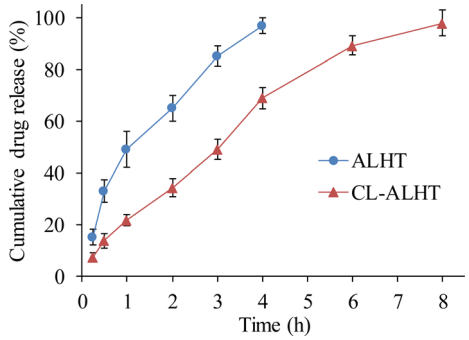

Fig. 9 VFX release from CL-ALHT and ALHT at pH 6.8.

The study regarding swelling/deswelling behavior of CL-ALH was also conducted in DW and ethanol. The CL-ALH showed good swelling in DW and deswelled in ethanol. The polarity and dielectric constant difference between DW and ethanol is the main cause of the swelling/deswelling behavior of CL-ALH in the corresponding medium. DW has more strong hydrogen bonding with CL-ALH as compared to ethanol which causes the reduction in ionization potential of the ionic groups of CL-ALH. Therefore, CL-ALH swells in DW and rapidly shrinks in ethanol.[41] Four cycles of these swelling/deswelling experiment of CL-ALH were performed (Fig. 8D). Additionally, it can be seen from the findings that CL-ALH deswells fully to its preliminary stage indicating the complete off/deswelling nature of the CL-ALH. Such findings show that patients should refrain from consuming alcohol-containing beverages when using a CL-ALH-based oral formulation because it may change the drug release profile.

Table 1 Kinetics data of VFX release from CL-ALHT and ALHT

Formulation code	Zero-order kinetics model		First-order kinetics model		Korsmeyer and Peppas model		
	R^2	K_0	R^2	K_1	R^2	K_{KP}	n
CL-ALHT	0.9669	12.238	0.9666	0.276	0.9860	23.079	0.720
ALHT	0.7585	27.786	0.9776	0.643	0.9877	45.245	0.559

3.8. Release of venlafaxine

As CL-ALH showed nearly off swelling behavior at gastric pH, *i.e.*, 1.2, therefore, the release experiment was performed at intestinal pH, *i.e.*, 6.8 mainly due to long transit time. The study of VFX release from CL-ALHT and ALHT showed that the release of VFX was completed in 8 h and 4 h, respectively. The sustained/prolonged release of VFX from CL-ALHT indicated its more sustained/prolonged release potential as compared to only ALHT. The release pattern of VFX from CL-ALHT followed the zero-order and first-order kinetics based on the value of R^2, *i.e.*, 0.9669 and 0.9666, respectively (Fig. 9; Table 1). Whereas, in case of ALHT, the VFX release only followed the first-order kinetics as the value of R^2 is 0.976. The mechanism of VFX release from CL-ALHT and ALHT followed the Korsmeyer and Peppas model based on the value of n, *i.e.*, 0.720 and 0.559, respectively which indicated the non-Fickian diffusion mechanism (Table 1).

3.9. X-ray study

The X-ray images of the CL-ALH tablet (ALHX) during transit through GIT are shown in Fig. 10. The image at 0 h indicated that the stomach was empty or free from any opaquant material. After the intake of the ALHX tablet, a bright and round image of the tablet can be seen till 2 h. During this period, the tablet is retained in the stomach of the dog. After that, the tablet moved to the intestine and started to swell and converted into fragments which resulted in a decrease in the size of the tablet. Hence, the decrease in the brightness and the reduction of the tablet size can be observed in the images captured after 5 and 7 h. After 7 h, the tablet disappears showing the complete disintegration of the ALHX tablet. These results indicated that the CL-ALH-based tablet can be recommended for the sustained release of active pharmaceutical ingredients. Moreover, such formulations can be recommended for small intestine or colon-targeted DDSs.

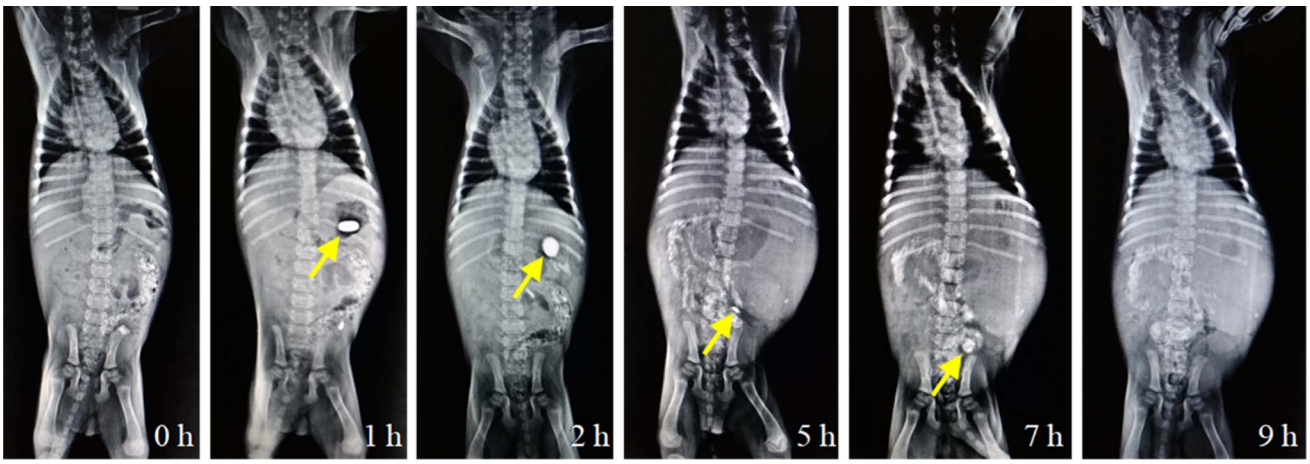

Fig. 10 X-ray images showing ALHX tablet transit through GIT of a stray dog.

4. Conclusion

Citric acid cross-linked *A. vera* leaves hydrogel (CL-ALH) was synthesized through esterification. The CL-ALH appeared a superporous material as revealed by SEM analysis. Such superporous materials are important to hold more fluids in their network structure and may offer on-demand/targeted drug release. Additionally, the pH-dependent swelling of CL-ALH made this novel material as an ideal candidate for targeted drug delivery applications. The high swelling in DW and at pH 6.8 and 7.4 opened up a new opportunity for targeted and site-specific applications, especially to the small intestine and colon. The CL-ALH showed admirable deswelling behavior at pH 1.2 which is good for keeping the stomach safe from the side effects of acidic drugs. On the other hand, acid-sensitive drugs can be kept safe from the harsh environment of the stomach. The less swelling ability of CL-ALH at pH 1.2 has also been witnessed through an X-ray study. The swelling of CL-ALH followed second-order kinetics. The drug release from CL-ALH-based tablets followed zero-order and first-order kinetics and non-Fickian diffusion mechanism. This indicated that CL-ALH is an intelligent material for the sustained release of drugs from tablet formulations.

Author contributions

Jaffar Irfan: investigation, methodology, writing – original draft. Arshad Ali: investigation, methodology, data curation, validation, writing – original draft. Muhammad Ajaz Hussain: conceptualization, supervision. Muhammad Tahir Haseeb: validation, writing – review & editing. Muhammad Naeem-ul-Hassan: supervision, Syed Zajif Hussain: data curation, investigation.

Conflicts of interest

There are no conflicts of interest to declare.

Acknowledgements

We are thankful to Dr Muhammad Umer Ashraf, University of Lahore, for providing the facility to conduct animal studies. We are deeply indebted to Dr Irfan Azhar, Southern University of Science and Technology, Shenzhen, 518055, China for the help in acquiring solid-state CP/MAS ^{13}C NMR analysis. We also acknowledge the radiology section of the Mubarak Medical Complex, Sargodha, Pakistan for the provision of X-ray analysis and expert opinion.

References

1 P. S. Nivedita, A. K. Shettar and H. H. Joy, Applications of polysaccharides in nutrition and medicine, in *Polysaccharides: Properties and Applications*, 2021, pp. 657–682, DOI: 10.1002/9781119711414.ch30.8.

2 Y. Yu, M. Shen, Q. Song and J. Xie, *Carbohydr. Polym.*, 2018, **183**, 91–101, DOI: 10.1016/j.carbpol.2017.12.009.

3 A. Ali, M. A. Hussain, M. T. Haseeb, M. U. Ashraf, M. Farid-ul-Haq, T. Tabassum, G. Muhammad and A. Abbas, *J. Braz. Chem. Soc.*, 2023, **34**, 906–917, DOI: 10.21577/0103-5053.20230001.

4 J. Pushpamalar, A. K. Veeramachineni, C. Owh and X. J. Loh, *ChemPlusChem*, 2016, **81**, 504–514, DOI: 10.1002/cplu.201600112.

5 A. S. A. Mohammed, M. Naveed and N. Jost, *J. Polym. Environ.*, 2021, **29**, 2359–2371, DOI: 10.1007/s10924-021-02052-2.

6 A. Dodero, S. Scarfi, S. Mirata, A. Sionkowska, S. Vicini, M. Alloisio and M. Castellano, *Polymers*, 2021, **13**, 831, DOI: 10.3390/polym13050831.

7 C. Alvarez-Lorenzo, B. Blanco-Fernandez, A. M. Puga and A. Concheiro, *Adv. Drug Delivery Rev.*, 2013, **65**, 148–1171, DOI: 10.1016/j.addr.2013.04.016.

8 M. A. Hussain, A. I. Rana, M. T. Haseeb, G. Muhammad and L. Kiran, *J. Drug Delivery Sci. Technol.*, 2020, **55**, 101470, DOI: 10.1016/j.jddst.2019.101470.

9 C. Alvarez-Lorenzo, B. Blanco-Fernandez, A. M. Puga and A. Concheiro, *Adv. Drug Delivery Rev.*, 2013, **65**, 1148–1171, DOI: 10.1016/j.addr.2013.04.016.

10 S. N. A. Bukhari, M. A. Hussain, M. T. Haseeb, A. Wahid, N. Ahmad, S. Z. Hussain, M. U. Munir and M. A. Elsherif, *Gels*, 2022, **8**, 283, DOI: 10.3390/gels8050283.

11 A. Ali, M. A. Hussain, M. T. Haseeb, S. N. A. Bukhari, T. Tabassum, M. Farid-ul-Haq and F. A. Sheikh, *J. Drug Delivery Sci. Technol.*, 2022, **69**, 103144, DOI: 10.1016/j.jddst.2022.103144.

12 A. Sood, A. Gupta and G. Agrawal, *Carbohydr. Polym. Technol. Appl.*, 2021, **2**, 100067, DOI: 10.1016/j.carpta.2021.100067.

13 M. Rinaudo, *Polym. Int.*, 2008, **57**, 397–430, DOI: 10.1002/pi.2378.

14 N. Reddy, R. Reddy and Q. Jiang, *Trends Biotechnol.*, 2015, **33**, 362–369, DOI: 10.1016/j.tibtech.2015.03.008.

15 A. C. Alavarse, E. C. G. Frachini, R. L. C. G. da Silva, V. H. Lima, A. Shavandi and D. F. S. Petri, *Int. J. Biol. Macromol.*, 2022, **202**, 558–596, DOI: 10.1016/j.ijbiomac.2022.01.029.

16 F. G. Mendonca, I. R. Menezes, I. F. Silva and R. M. Lago, *New J. Chem.*, 2021, **45**, 2410–2416, DOI: 10.1039/D0NJ06138G.

17 M. A. Hussain, L. Kiran, M. T. Haseeb, I. Hussain and S. Z. Hussain, *J. Polym. Res.*, 2020, **27**, 1–10, DOI: 10.1007/s10965-020-2025-9.

18 R. Moriana, Y. Zhang, P. Mischnick, J. Li and M. Ek, *Carbohydr. Polym.*, 2014, **106**, 60–70, DOI: 10.1016/j.carbpol.2014.01.086.

19 J. H. Hamman, *Molecules*, 2008, **13**, 599–1616, DOI: 10.3390/molecules13081599.

20 P. Venkataharsha, E. Maheshwara, Y. P. Raju, V. A. Reddy, B. S. Rayadu and B. Karisetty, *Int. J. Pharm. Invest.*, 2015, **5**, 28–34, DOI: 10.4103/2230-973X.147230.

21 A. Mahmood, A. Erum, U. R. Tulain, S. Shafiq, N. S. Malik, Sidra, M. T. Khan and M. S. Alqahtani, *Gels*, 2023, **9**, 474, DOI: 10.3390/gels9060474.

22 A. Balaji, M. V. Vellayappan, A. A. John, A. P. Subramanian, S. K. Jaganathan, M. SelvaKumar, A. A. bin Mohd Faudzi, E. Supriyanto and M. Yusof, *RSC Adv.*, 2015, **5**, 86199–86213, DOI: **10.1039/C5RA13282G**.

23 A. Laux, C. Gouws and J. H. Hamman, *Drug Delivery*, 2019, **16**, 1283–1285, DOI: **10.1080/17425247.2019.1675633**.

24 D. Massoud, B. M. Alrashdi, M. Fouda, A. El-kott, S. A. Soliman and H. H. Abd-Elhafeez, *Braz. J. Pharm. Sci.*, 2022, **58**, e20837, DOI: **10.1590/s2175-97902022e20837**.

25 M. Chelu, A. M. Musuc, M. Popa and J. Calderon Moreno, *Gels*, 2023, **9**, 539, DOI: **10.3390/gels9070539**.

26 M. U. Ashraf, M. A. Hussain, S. Bashir, M. T. Haseeb and Z. Hussain, *J. Drug Delivery Sci. Technol.*, 2018, **45**, 455–465, DOI: **10.1016/j.jddst.2018.04.008**.

27 M. Gibaldi and S. Feldman, *J. Pharm. Sci.*, 1967, **56**, 1238–1242, DOI: **10.1002/jps.2600561005**.

28 R. W. Korsmeyer, R. Gurny, E. Doelker, P. Buri and N. A. Peppas, *Int. J. Pharm.*, 1983, **15**, 25–35, DOI: **10.1016/0378-5173(83)90064-9**.

29 P. I. Ritger and N. A. Peppas, *J. Controlled Release*, 1987, **5**, 37–42, DOI: **10.1016/0168-3659(87)90035-6**.

30 J. Siepmann and N. A. Peppas, *Adv. Drug Delivery Rev.*, 2001, **48**, 137–138, DOI: **10.1016/S0169-409X(01)00111-9**.

31 C. Demitri, R. Del Sole, F. Scalera, A. Sannino, G. Vasapollo, A. Maffezzoli, L. Ambrosio and L. Nicolais, *J. Appl. Polym. Sci.*, 2008, **110**, 2453–2460, DOI: **10.1002/app.28660**.

32 J. Irfan, A. Ali, M. A. Hussain, A. Abbas, M. T. Haseeb, M. Naeem-ul-Hassan, I. Azhar, S. Z. Hussain and I. Hussain, *Int. J. Biol. Macromol.*, 2024, **259**, 128879, DOI: **10.1016/j.ijbiomac.2023.128879**.

33 A. Ali, M. A. Hussain, A. Abbas, M. T. Haseeb, I. Azhar, G. Muhammad, S. Z. Hussain, I. Hussain and N. F. Alotaibi, *J. Mol. Liq.*, 2023, **376**, 121438, DOI: **10.1016/j.molliq.2023.121438**.

34 A. A. Keirudin, N. Zainuddin and N. A. Yusof, *Polymers*, 2020, **12**, 2465, DOI: **10.3390/polym12112465**.

35 B. A. Lodhi, M. A. Hussain, M. U. Ashraf, M. T. Haseeb, G. Muhammad, M. Farid-ul-Haq and M. Naeem-ul-Hassan, *Ind. Crops Prod.*, 2020, **155**, 112780, DOI: **10.1016/j.indcrop.2020.112780**.

36 S. Hajebi, A. Abdollahi, H. Roghani-Mamaqani and M. Salami-Kalajahi, *Polymer*, 2019, **180**, 121716, DOI: **10.1016/j.polymer.2019.121716**.

37 S. Hajebi, A. Abdollahi, H. Roghani-Mamaqani and M. Salami-Kalajahi, *Langmuir*, 2020, **36**, 2683–2694, DOI: **10.1021/acs.langmuir.9b03892**.

38 A. Ali, M. A. Hussain, M. T. Haseeb, U. R. Tulain, M. Farid-ul-Haq, T. Tabassum, G. Muhammad, S. Z. Hussain, I. Hussain and A. Erum, *React. Funct. Polym.*, 2023, **182**, 105466, DOI: **10.1016/j.reactfunctpolym.2022.105466**.

39 B. Razavi, A. Abdollahi, H. Roghani-Mamaqani and M. Salami-Kalajahi, *Mater. Sci. Eng., C*, 2020, **109**, 110524, DOI: **10.1016/j.msec.2019.110524**.

40 B. Razavi, A. Abdollahi, H. Roghani-Mamaqani and M. Salami-Kalajahi, *Polymer*, 2020, **187**, 122046, DOI: **10.1016/j.polymer.2019.122046**.

41 A. Ali, M. A. Hussain, M. T. Haseeb, S. N. A. Bukhari, G. Muhammad, F. A. Sheikh, M. Farid-ul-Haq and N. Ahmad, *Curr. Drug Delivery*, 2023, **20**, 292–305, DOI: **10.2174/1567201819666220509200019**.